Sustainable Energy Technologies and Assessments 72 (2024) 104031

Contents lists available at ScienceDirect

Sustainable Energy Technologies and Assessments

journal homepage: www.elsevier.com/locate/seta

Original article

# Developing solar vacuum cylindrical cavity receiver for reducing $CO_2$ Pollutant: A new approach to energy governance

Reyhaneh Loni [a,*], Alibakhsh Kasaeian [b], Mohsen Sharifpur [c,d,*], Gholamhassan Najafi [e]

[a] Department of Energy Governance, Faculty of Governance, University of Tehran, 14398-14151, Tehran, Iran
[b] Department of Renewable Energies, Faculty of New Sciences & Technologies, University of Tehran, Tehran, Iran
[c] School of Mechanical, Industrial and Aeronautical Engineering, University of the Witwatersrand, Private Bag 3, Wits 2050, South Africa
[d] Department of Medical Research, China Medical University Hospital, China Medical University, Taichung, Taiwan
[e] Department Mechanic of Biosystems Engineering, Tarbiat Modares University, Tehran, Iran

ARTICLE INFO

*Keywords:*
Solar energy
Vacuum cavity receiver
$Co_2$ emission
Organic Rankine Cycle (ORC)
Energy Governance
Policy design

ABSTRACT

Air pollution is recognized as a critical environmental challenge impacting humanity, with factors such as population growth, industrial expansion, and increased use of motorized vehicles contributing to its worsening. Presently, developing nations like Iran, particularly cities such as Tehran, grapple with severe air pollution issues exacerbated by the heavy reliance on fossil fuels. This research introduces a solar power system integrating an Organic Rankine Cycle (ORC) unit to generate electricity while concurrently addressing air pollution concerns. A novel solar dish concentrator featuring a vacuum cylindrical cavity receiver was studied optically and thermally in Tehran, Iran, from 2001 to 2022. The investigation also analyzed the emission reduction potential and land requirements for implementing the solar ORC system. The results indicated that employing the ORC system with a vacuum cavity receiver offers a more effective solution for reducing $CO_2$ emissions and enhancing environmental conditions. To satisfy 10% of Tehran's industrial power demand in 2022, the solar ORC system required about 459 ha of land for the vacuum cylindrical receiver, whereas the non-vacuum cylindrical receiver necessitated approximately 538 ha. In essence, developing this solar ORC system could lead to a carbon mitigation of 1,676,641.50 tons of $CO_2$ and generate carbon credits valued at $24,311,287.31. Ultimately, the proposed solar ORC system holds significant promise in advancing energy governance by establishing innovative power plant systems.

## Introduction

For many years, the energy crisis and urban pollution have presented urgent challenges [1]. The rapid population growth and societal advancements necessitate a reassessment of our energy supply sources [2]. An in-depth analysis underscores the global significance of the critical challenges posed by the energy crisis and environmental pollution resulting from our heavy reliance on fossil fuels [3]. While the use of fossil fuels like coal, oil, and gas has surged, the finite nature of these resources and their impact on environmental issues such as global warming, melting ice caps, and ecological disruptions highlight the necessity for alternative energy sources [4]. Renewable energy (RE) sources have emerged as viable solutions to address these issues, offering reduced emissions and fewer constraints [5].

In recent decades, significant progress has been achieved in advancing RE technologies, encompassing solar, wind, water, geothermal, bioenergy, hydrogen, and fuel cell technologies [6,7]. The escalating energy crisis and heightened environmental consciousness, exemplified by initiatives like the Kyoto Protocol aimed at reducing $CO_2$ emissions, have prompted countries to adopt new approaches to energy management [8]. This shift from fossil fuels to RE sources has become imperative for reducing energy consumption, balancing supply and demand, and mitigating harmful emissions [9]. The transition to renewable energies is critical for pollution mitigation and offers long-term economic advantages through cost savings and a more sustainable energy outlook. Regarding RE applications, solar systems are particularly popular and widely utilized for electricity generation [10].

Solar Energy (SE) is widely recognized as a leading RE source on a global scale [11]. Solar power offers a sustainable and eco-friendly alternative to conventional energy sources by harnessing sunlight to generate electricity. Its sustainability and dependability make it a

* Corresponding authors at: Department of Energy Governance, Faculty of Governance, University of Tehran, 14398-14151, Tehran, Iran (R. Loni).
*E-mail addresses:* rloni@ut.ac.ir (R. Loni), mohsen.sharifpur@wits.ac.za (M. Sharifpur).

https://doi.org/10.1016/j.seta.2024.104031
Received 21 July 2024; Received in revised form 30 September 2024; Accepted 13 October 2024
Available online 22 October 2024
2213-1388/© 2024 Elsevier Ltd. All rights are reserved, including those for text and data mining, AI training, and similar technologies.

**Nomenclature**

| | |
|---|---|
| A | area, $m^2$ |
| $c_2$ | constant |
| $c_p$ | constant pressure specific heat, J/kgK |
| d | receiver tube diameter, m |
| D | cavity aperture diameter, m |
| $\dot{E}$ | exergy |
| $F$ | view factor |
| $f_r$ | Friction factor |
| h | cavity depth, m |
| $h^*$ | enthalpy, kJ/kg |
| $h'$ | heat transfer coefficient, $W/m^2K$ |
| $I_{sun}$, $G$ | solar irradiance ($W/m^2$) |
| $k$ | thermal conductivity, W/mK |
| $m_2$ | slope of linear equation |
| $\dot{m}$ | mass flow rate, kg/s |
| $N$ | number of tube sections |
| Nu | Nusselt number |
| $\dot{Q}_{net}$ | net heat transfer rate, W |
| $\dot{Q}^*$ | rate of available solar heat at receiver cavity, W |
| $\dot{Q}_{loss}$ | loss rate of heat loss from the cavity receiver, W |
| $\dot{Q}_{solar}$ | 0258, W |
| P | pressure (KPa) |
| Pr | Partner number |
| $q$ | heat (kJ/kg) |
| $R$ | thermal resistance, K/W |
| Re | Reynolds number |
| $T$ | Temperature, K |
| TIT | Turbine Inlet Temperature, K |
| $\dot{W}$ | power, W |

*Greek symbols*

| | |
|---|---|
| $\varepsilon$ | emissivity |
| $\sigma$ | Stefan–Boltzmann constant, $W/m^2K$ |
| $\eta$ | efficiency |
| $\omega$ | error |
| $\varphi_{CO_2}$ | annual $CO_2$ emissions, ton |
| $\psi_{CO_2}$ | average $CO_2$ emissions from coal power production, $kgCO_2/kWh$ |
| $E_{en,ann}$ | electricity generated by the solar or ORC systems over a year, kWh |
| $Z_{CO_2}$ | carbon credit, $ |
| $z_{CO_2}$ | carbon credit, $ per ton |

*Subscripts*

| | |
|---|---|
| *0, in* | *initial inlet to receiver* |
| *ab* | *absorption* |
| *amb* | *ambient* |
| *ap* | *aperture* |
| *Ave* | *average* |
| *b* | *boiler* |
| *bp* | *boiling point* |
| *cav* | *for the cavity* |
| *col* | *overall for the collector* |
| *conc* | *concentrator* |
| *cond* | *due to conduction* |
| *conv* | *due to convection* |
| *cr* | *critical* |
| *Dish* | *dish concentrator* |
| *evp* | *evaporator* |
| *exergy* | *exergy* |
| *f* | *fluid* |
| *F* | *factor* |
| *gained* | *gained* |
| *inlet* | *at the inlet* |
| *loss* | *loss* |
| *n* | *tube section number* |
| *oil* | *thermal oil* |
| *optical* | *optical* |
| *out, outlet* | *at the outlet* |
| *outer* | *out of the cavity* |
| *PUMP* | *pump* |
| *rec, R* | *receiver* |
| *rad* | *due to radiation* |
| *s* | *surface of the inner tube* |
| *slop* | *slop* |
| *specularity* | *specularity* |
| *sun* | *sun* |
| *t* | *turbine* |
| *th* | *thermal* |
| *tube* | *tube* |
| *walls* | *cavity walls* |
| $\infty$ | *environment* |

*Abbreviation*

| | |
|---|---|
| CRs | cavity receivers |
| DNI | direct normal irradiance |
| LCOE | levelized cost of electricity |
| LFR | linear Fresnel reflector |
| MCFC | molten carbonate fuel cell |
| NREL | National Renewable Energy Laboratory |
| ORC | Organic Rankine Cycle |
| PDC | parabolic dish collector |
| RE | Renewable energy |
| SDGs | sustainable development goals |
| SE | Solar Energy |
| UNCED | United Nations Conference on Environment and Development |

popular choice for individuals seeking a long-term, environmentally conscious energy solution [12]. The technologies available for converting SE into electrical power are typically categorized as direct or indirect methods [13]. Direct solar methods involve the use of photovoltaic systems to convert SE into electricity directly [14]. Indirect solar techniques, on the other hand, encompass the utilization of solar thermal power plants, which convert absorbed thermal energy into electrical power [15]. In every solar thermal power plant, a thermodynamic cycle known as a power cycle operates to produce useful work [16]. This power cycle necessitates a working fluid that circulates through the equipment, transferring energy as a medium. An Organic Rankine Cycle (ORC) system is a type of power plant that utilizes an organic working fluid for generating power [17]. The ORC system is capable of producing power at low to medium temperatures by leveraging the saturation and super-saturation properties of organic fluids at lower temperatures. Additionally, SE can serve as the heat source for an ORC system [18].

Researchers have explored solar systems as a means to reduce air pollution through both numerical and experimental approaches. Motlagh et al. [19] introduced a new model to assess solar systems' air pollution reduction potential, focusing on PV and PV/T technologies in Tehran, Iran. Their research aimed to provide energy decision-makers with valuable insights for informed choices, highlighting SE systems as effective tools for air pollution mitigation. In a comprehensive review, Liu et al. [20] discussed strategies for reducing air pollution using solar chimneys. They examined various geoengineering methods involving solar chimneys to address future air quality issues, particularly concerning suspended particles. Hachicha et al. [21] conducted a numerical evaluation and optimization of a novel hybrid solar chimney design as a promising technology for air pollution reduction. Their study focused on the impact of an innovative filter-equipped solar chimney collector structure on system performance in reducing air pollution, achieving remarkable results with 28.3 kW generation at 90.5 % filter efficiency. Manrique and Villaseñor [22] investigated the effects of inclined planes exposed to solar radiation on building roofs in reducing air pollution, utilizing both numerical simulations and experimental analyses. Additionally, Yang et al. [23] studied the influence of air pollution on global and diffuse solar radiation in six selected cities in China from 2014 to 2020 under clear sky conditions. Overall, the application of SE for power generation emerges as a promising solution for air pollution reduction.

Researchers have extensively explored solar ORC systems as an efficient option for power generation [24–26]. Solar ORC systems are a promising solution for converting solar energy into electricity. These systems use organic fluids with low to medium boiling points to facilitate efficient energy conversion. Morid and Khoshgoftar Manesh [27] developed an integrated poly-generation system that merges fossil fuel and solar energy to fulfill various needs, including electricity generation, cooling, heating, freshwater production, and CO2 capture. The results indicated notable advancements as freshwater production increases by 95.25 %, fuel consumption decreases by 22 %, and net power generation of the GTC rises by 5 %. The overall energy efficiency was reported at 34.27 % for single generation (power alone) and 65.65 % for multiple generation. Ghorbani et al. [28] addressed the rising global energy demand by developing an innovative hybrid system for cogeneration of electricity and desalinated water, emphasizing maximum efficiency through thermal integration. The proposed hybrid system incorporated an organic Rankine unit, a carbon dioxide power plant, a Kalina power cycle utilizing seawater temperature differences, and a multi-effect desalination system, with part of the necessary heat supplied by solar flat plate collectors. Mei et al. [29] analyzed the performance of a hybrid energy system that combines a molten carbonate fuel cell (MCFC), parabolic dish collector (PDC), linear Fresnel reflector (LFR), Organic Rankine Cycle (ORC), gas turbine, and an integrated carbon dioxide separation process. The proposed system utilized waste heat from the MCFC to enhance electricity generation in the ORC and incorporates both LFR and PDC for efficient heating. The LFR elevated water temperatures before fuel mixing, while the PDC further heats the mixture prior to entering the reformer. The study also investigated the role of the parabolic trough collector in supplying the evaporator's thermal duty for the ORC.

Rahmdel et al. [18] developed a real-time model for electricity, water production, and high-temperature heating energy using a solar ORC system, demonstrating positive outcomes over two typical days in Zahedan, Iran. In a thermoeconomic evaluation, Fan et al. [30] assessed a solar ORC system as a bottoming cycle subsystem, revealing a payback period of 6 years and a levelized cost of electricity (LCOE) of $0.07/kWh in regions with high direct normal irradiance (DNI). Shahverdi et al. [31] investigated a solar ORC system integrated with a micro hydropower system for power generation, analyzing the impact of different system parameters on performance. They reported an efficiency of 58.24 % for the hybrid power system.

Refiei et al. [32] conducted a study on a solar ORC system utilizing carbon nanoparticles in thermal oil as the solar working fluid. They employed a solar dish concentrator with cavity receivers (CRs) as the heat source for the ORC system, achieving a performance efficiency of 21.4 %. In a review paper, Loni et al. [33] identified the solar ORC system with a solar parabolic trough concentrator as the most effective for power generation. Shahverdi et al. [34] proposed and assessed a novel water pump system integrated with a solar ORC system, with a solar parabolic trough concentrator serving as the heat source. Their system exhibited a collector efficiency of 47.85 %, thermodynamic efficiency of 27.46 %, and storage efficiency of 92.72 % in the optimal design. Researchers have explored solar ORC systems with various CR shapes to enhance thermal performance and minimize heat losses [35]. Loni et al., in multiple studies, evaluated solar ORC systems utilizing CRs [17,36], employing solar dish concentrators and parabolic trough concentrators as heat sources. Their analyses indicated satisfactory performance of the solar ORC systems based on thermodynamic assessments.

The literature review suggests that utilizing solar systems is a promising technology for reducing air pollution. This study introduced a groundbreaking solar ORC system, featuring a novel vacuum cylindrical CR design integrated with a solar dish concentrator. In other words, suggestion and developing a solar dish concentrator with a cylindrical cavity receiver is presented as the main novelty of this study compared to other researches. The solar system was developed as heat source of the ORC system for power generation. Subsequently, analyses were conducted as a case study to evaluate emission reduction levels and land requirements for implementing the solar ORC system in Tehran, Iran. Additionally, the study discusses how to enhance energy governance by improving the proposed power plant systems. The findings of this research can assist governments in making informed policy decisions to promote the use of solar energy.

## Methodology

### *Solar ORC modeling*

The rise in global energy resource consumption has depleted reserves and contributed to environmental pollution. RE sources, such as SE, geothermal energy, and waste heat from industrial processes, offer a promising alternative to traditional energy sources. The Organic Rankine Cycle (ORC) is recognized as a viable technology for converting thermal energy into electricity from low-temperature heat sources using organic fluids as the working medium. This study examined a solar dish concentrator with a cylindrical CR as the heat source for an ORC system. Initially, the solar system was simulated using SolTrace and Maple software in the research's initial phase.

The optical simulation of the solar dish concentrator was conducted using the SolTrace software. Developed by the National Renewable Energy Laboratory (NREL), SolTrace is utilized for optical modeling and functional analysis of solar collector systems. This software employs the Monte Carlo method for the optical modeling of concentrator collectors and is highly recommended as a freely available tool to assess the optical performance of solar power generation systems with reliable accuracy [37]. The calculation of optical error in the SolTrace software is determined by the following equation:

$$\omega_{optical} = \left(4\omega_{slop}^2 + \omega_{specularity}^2\right)^{1/2} \tag{1}$$

This formula combines the contributions of slope error ($\omega_{slop}$) and, specularity error ($\omega_{specularity}$) to determine the overall optical error ($\omega_{optical}$). In this study, the sun's shape was represented using the pillbox method, with 1000 radiations utilized for optical modeling of the plate solar collector. Conversely, the solar collector at Tarbiat Modares University in Tehran, Iran, was modeled with an inlet diameter of 1.8 m and a collector angle of 45°. The optical efficiency of the CR, simulated in the SolTrace software, can be determined using Equation 2. This equation will also be applied in the forthcoming research to assess the optical efficiency of the receiver [38].

$$\eta_{optical} = Q_{abs,walls} / Q_{rec,dish} \tag{2}$$

The equation defines $\eta_{optical}$ as the optical efficiency, $Q_{abs,walls}$ (W) as the heat absorbed by the cylindrical cavity walls, and $Q_{rec,dish}$ (W) as the total solar radiation received by the dish concentrator. It should be mentioned that the calculation of optical efficiency is vital for optimizing design, enhancing performance, and ensuring the economic viability of solar energy systems. The solar system's thermal modeling was conducted through coding in the Maple software. The methodology employed in this study is well-suited for basic solar receiver modeling, with a more comprehensive approach taken into consideration, encompassing various factors. Each receiver coil is treated as an individual element with a specific surface temperature and net heat transfer rate. Fig. 1 displays a summary of the developed thermal modeling based on writing codes in the Maple software. The numerical model developed is elaborated upon below, with the surface temperature ($T_{s,n}$) and net heat transfer rate ($\dot{Q}_{net,n}$) at different tube sections computed by solving Equations **(3)** and **(8)** utilizing the Newton–Raphson Method as outlined [35]:

$$\dot{Q}_{net,n} = \frac{\left(T_{s,n} - \sum_{i=1}^{n-1}\left(\frac{\dot{Q}_{net,i}}{\dot{m}c_{p0}}\right) - T_{inlet,0}\right)}{\left(\frac{1}{h_{inner}A_n} + \frac{1}{2\dot{m}c_{p0}}\right)} \tag{3}$$

This equation computes the net heat transfer rate ($\dot{Q}_{net,n}$) at different tube sections in a thermal system. In this Eq., $\dot{Q}_{net,n}$ (W) is the net heat transfer rate at the n-th tube section, *Ts,n* (°C) is surface temperature of the tube at the n-th section, *T*inlet,0 (°C) is inlet temperature of the fluid at the beginning of the system (0-th section), $\dot{m}$(kg/s) is mass flow rate of the fluid, $c_{p0}$(J/(kg·K) is specific heat capacity of the fluid at the inlet conditions, *h*inner (W/(m$^2$·K)) is Convective heat transfer coefficient on the inner surface of the tube, and *An* (m$^2$) is Surface area of the tube at the *n*-th section.

The equation for ($Nu_{inner}$) leverages the interplay of friction, inertia, and thermal properties of the working fluid to predict the efficiency of convective heat transfer in an internal flow scenario, which is crucial for the design and optimization of systems such as heat exchangers, pipes, and cooling systems. Understanding these parameters helps engineers make informed decisions to enhance performance and reliability in fluid transport and thermal management applications. The Nusselt number for the internal working fluid flow is approximated as follows [35]:

$$Nu_{inner} = \frac{\left(\frac{f_r}{8}\right)\cdot Re\cdot Pr}{1 + 12.8\cdot\sqrt{\frac{f_r}{8}}\cdot\left(Pr^{0.68} - 1\right)} \tag{4}$$

In this equation, $Nu_{inner}$ is a dimensionless number representing the ratio of convective to conductive heat transfer. A higher Nu indicates better heat transfer. The $f_r$ is the Darcy–Weisbach friction factor, which quantifies the pressure drop due to friction in a fluid flowing through a pipe or duct. It is affected by the flow regime (laminar or turbulent) and the roughness of the pipe. The *Re* is a dimensionless number that provides insight into the flow regime of the fluid (laminar or turbulent). It is a ratio of inertial forces to viscous forces. The *Pr* is a dimensionless number that represents the ratio of momentum diffusivity to thermal diffusivity. It measures the relative thickness of the thermal and velocity boundary layers. The friction factor ($f_r$) is determined by:

$$f_r = (0.79\ln Re - 1.64)^{-2} \tag{5}$$

This equation calculates the friction factor used in fluid mechanics, particularly in internal flow analysis, such as flow in pipes or ducts. In this equation, $f_r$ is the Darcy–Weisbach friction factor, which is dimensionless. It quantifies the resistance to flow due to friction in a fluid moving through a pipe or duct. *Re* is The Reynolds number, which is a dimensionless quantity used to predict flow patterns in different fluid flow situations. It is defined as the ratio of inertial forces to viscous

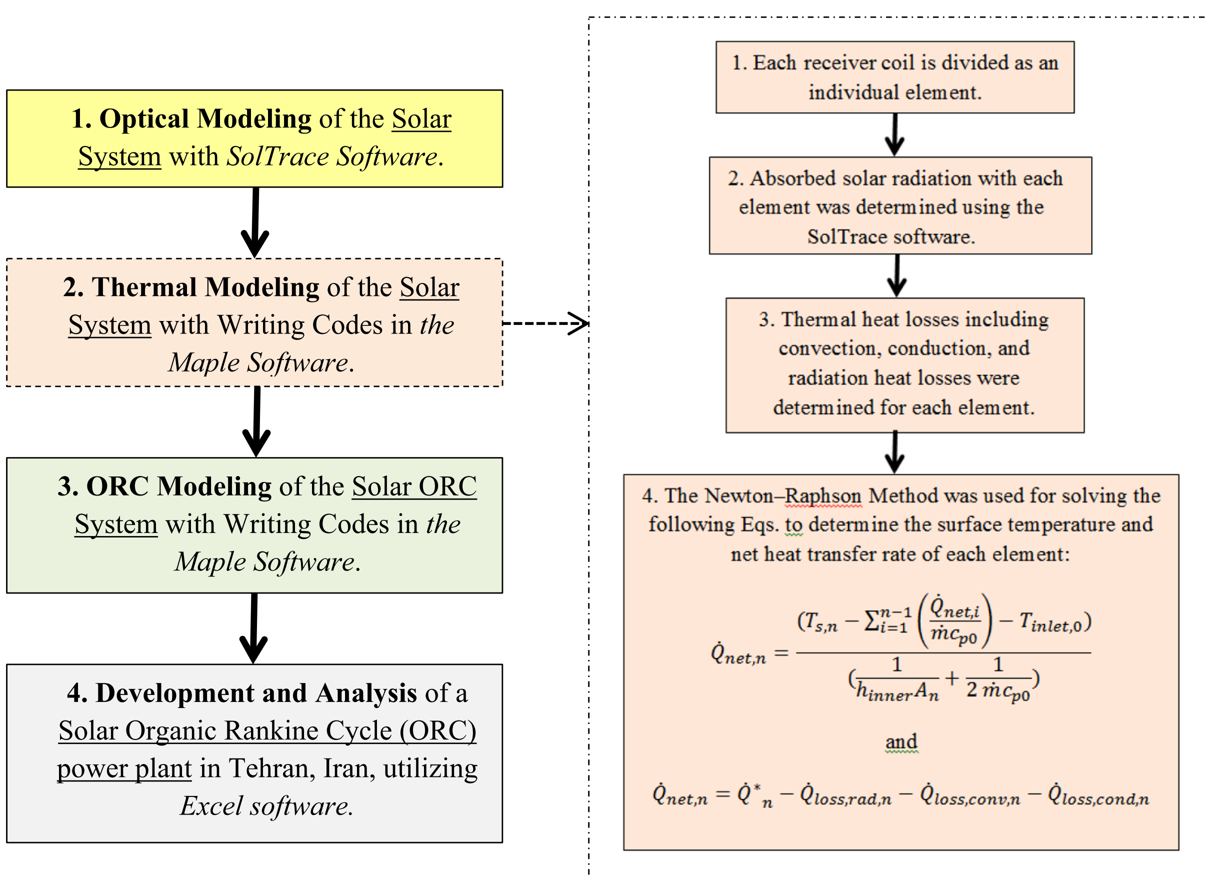


**Fig. 1.** A flowchart of the analysis process during the study in summary way.

forces and is a key parameter in determining whether flow is laminar or turbulent. Additionally, the net heat transfer coefficient is assessed by [38]:

$$h'_{inner} = \frac{Nu_{inner} \cdot k_f}{d_{tube}} \quad (6)$$

This equation is critical in thermal engineering, especially in designing heat exchangers, cooling systems, and other applications where fluid heat transfer is involved. Understanding the heat transfer coefficient allows engineers to analyze thermal performance and optimize designs for efficiency. In this equation, the $h_{inner}$ $\left(\mathrm{W}/\left(\mathrm{m}^2\cdot\mathrm{K}\right)\right)$ is the heat transfer coefficient quantifies the heat transfer rate per unit area per unit temperature difference between a solid surface and a fluid. It's a crucial parameter in determining how effectively heat is transferred to or from a fluid flowing inside a tube. The $Nu_{inner}$ is the Nusselt number indicates the enhancement of heat transfer through a fluid as a result of convection relative to conduction. It incorporates fluid properties and flow characteristics. The $k_f$ (W/(m·K)) is thermal conductivity is a measure of a material's ability to conduct heat. For fluids, it indicates how well the fluid can transfer heat. This value typically varies based on the fluid type and its temperature. $d_{tube}$ (m) is the hydraulic diameter or inner diameter of the tube through which the fluid flows. The diameter significantly influences the flow conditions and consequently the heat transfer characteristics. The net heat transfer rate can be calculated using the following equations [38]:

$$\dot{Q}_{net,n} = \dot{Q}^*_n - \dot{Q}_{loss,rad,n} - \dot{Q}_{loss,conv,n} - \dot{Q}_{loss,cond,n} \quad (7)$$

$$\dot{Q}_{net,n} = \dot{Q}^*_n - A_n\varepsilon_n\sigma\left(T_{s,n}{}^4\right) + A_n\sum_{j=1}^{N}F_{n-j}\varepsilon_j\sigma\left(T_{s,n}{}^4\right) - A_n\varepsilon_n\sigma F_{n-\infty}T_\infty^4 - A_n\left(m_2T_{s,n}+c_2\right) - \frac{A_n}{R_{cond}}\left(T_{s,n}-T_\infty\right) \quad (8)$$

Both equations stem from the physical principles of energy balance and thermal transfer. They account for the heat added to a section and various modes of heat loss—radiative, convective, and conductive. The net heat transfer rate is critical in systems like heat exchangers, where understanding and optimizing heat transfer is central to design and efficiency. By using these equations iteratively for different sections of a tube or heat exchanger, one can model how heat moves through the system, leading to better thermal management solutions.

About Eq. 7, $\dot{Q}_{net,n}$ (W) is the overall amount of heat transferred out or into a section of a system. The $\dot{Q}^*_n$ (W) is the total received heat energy being added to section "n" of the system that calculated by the SolTrace software. The $\dot{Q}_{loss,rad,n}$ (W) is the amount of heat lost due to radiation from the surface of the section "n". The amount of $\dot{Q}_{loss,conv,n}$ (W) is the heat lost from section "n" to the surrounding fluid due to convection. And, the $\dot{Q}_{loss,cond,n}$ (W) is The heat lost through conduction from section "n" to adjacent materials.

About Eq. 8, $A_n$ ($\mathrm{m}^2$) is the surface area of section "n" where heat transfer occurs. The $\varepsilon_n$ is the measure of a material's ability to emit energy as thermal radiation; varies from 0 (perfect reflector) to 1 (perfect emitter). The $\sigma$ ($\mathrm{W}/(\mathrm{m}^2\mathrm{K}^4)$) is a physical constant used in the Stefan-Boltzmann law, which relates the power radiated by a black body to its temperature. The $T_{s,n}$ (K) is the temperature at the surface of section "n". The amount of $F_{n\text{-}j}$ is a measure of how much of the radiation leaving surface "n" reaches surface "j". $T_\infty$ (K) is the ambient temperature far from the surface of section "n". The $R_{cond}$ (K/W) is a measure of a material's ability to resist heat transfer; it is used in conductive heat loss calculations. More details related to these Eqs. have been presented by first author and et al. in Ref. [25].

The net heat transfer rate can be computed using the provided equations. Following the calculation of the effective net heat transfer rate ($\dot{Q}_{net,n}$) at different tube sections, the thermal efficiency of the examined CR is then determined by [38]:

$$\eta_{th} = \sum_{n=1}^{N}\frac{\dot{Q}_{net,n}}{\dot{Q}_{solar}} \quad (9)$$

It is important to emphasize that each receiver coil is considered a separate element in the current modeling methodology. The thermal modeling schematic of the cylindrical CR is illustrated in Fig. 2a. Further insights into the thermal analyses of the cylindrical CR can be found in the work by Loni et al. Notably, this study evaluated vacuum and non-vacuum cylindrical CRs for the first time globally. Internal convection heat losses were assumed to be zero for the vacuum configuration of the CR.

As previously mentioned, the solar system was utilized as the heat source for an ORC system designed for power generation. In this setup, the solar working fluid absorbs heat, which is then transferred to an organic fluid in the evaporator unit of the ORC system. Subsequently, the superheated organic fluid is directed to the turbine unit for power generation. Following this, the organic fluid undergoes a phase change in the condenser unit of the ORC system. Finally, a pump circulates the organic fluid within the ORC system. A schematic representation of the solar ORC system is provided in Fig. 2b. The ORC efficiency was calculated by the following equation [39]:

$$\eta_{ORC} = \frac{W_{net}}{Q_b} = \frac{W_t - W_{PUMP}}{Q_b} = \frac{m_f(h^*_3 - h^*_4) - m_f(h^*_2 - h^*_1)}{m_f(h^*_3 - h^*_2)} \quad (10)$$

Where $\eta_{ORC}$ is the ORC efficiency, $W_{net}$(W) is the net power output and $Q_b$ (W) is the absorbed heat energy by the evaporator. The flow rate of the organic fluid can be defined as follows [39]:

$$m_f = \frac{m_{oil}c_p(T_{out} - T_{in})}{(h^*_3 - h^*_2)} \quad (11)$$

Where defined based on the absorbed heat by the solar system. Propane was used as the ORC working fluid at a constant turbine inlet pressure of 3 MPa, and constant condenser temperature of 38 °C The use of propane was chosen for the solar-ORC setup based on recommendations from Ref. such as [33,40,41] and low critical temperature (96.7 °C) based on the condition of the solar-ORC system. Also, the critical pressure of Propane is 4.25 Mpa [41], so that constant turbine inlet pressure of 3 MPa was selected. In this study, thermodynamic properties were computed using REFPROP.8 software developed by NIST. The study concentrated on assessing the efficiency of the Organic Rankine Cycle (ORC) system, which comprises the evaporator, turbine, condenser, and pump. It should be mentioned that the ORC modeling was conducted using codes written in Excel software. Neglecting pressure drops in the heat exchangers and pipelines as well as any heat losses from the pipelines.

Exergy analysis is crucial for studying energy systems, particularly for concentrating collectors that are commonly linked to power cycles for generating power. In practice, this analysis assesses the useful heat production amount and operating temperature to determine the potential work output margin. The sun temperature ($T_{sun}$) has been chosen as 5800 K. The exergy of the solar irradiation can be expressed as [42]:

$$\sum \dot{E}_{in,rec} = \eta_p \cdot I_{solar} \cdot A_{conc} \quad (12)$$

Where:

$$\eta_p = 1 - \frac{4}{3}\cdot\frac{T_\infty}{3T_{sun}} + \frac{1}{3}\cdot\left(\frac{T_\infty}{T_{sun}}\right)^4 \quad (13)$$

The useful exergy production of the collector is determined by the following equation [42]:

$$\sum \dot{E}_{gain} = \dot{m}\cdot C_p\cdot\left(T_{outlet} - T_{inlet} - T_\infty \ln\left(\frac{T_{outlet}}{T_{inlet}}\right)\right) - \frac{T_\infty}{T_f}\frac{\dot{m}\Delta P}{\rho} \quad (14)$$

 

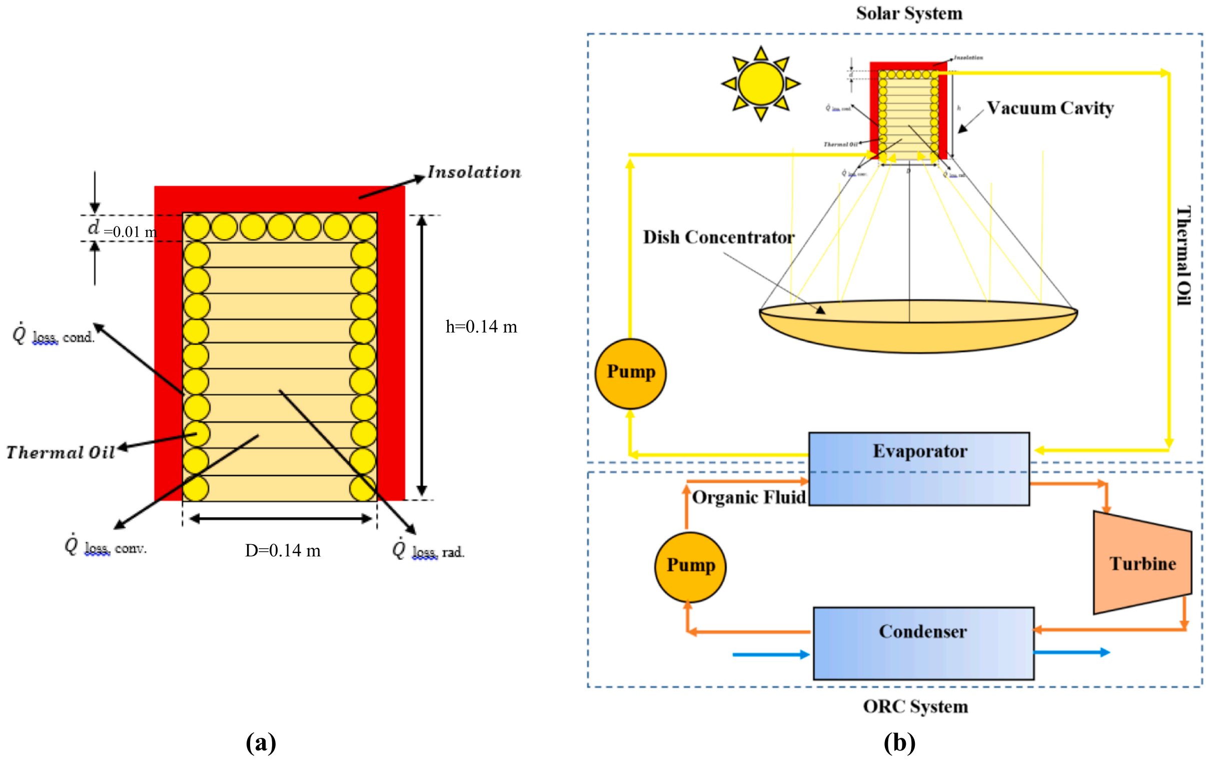


**Fig. 2.** A schematic view of a) the cylindrical CR for the thermal modeling, and the solar ORC system.

The exergetic efficiency of the collector can be defined as the ratio of the useful exergy production to the exergy input from the sun, as indicated by the following Equation [42]:

$$\eta_{exergy} = \frac{\sum \dot{E}_{gain}}{\sum \dot{E}_{in,rec}} \quad (15)$$

*Emission analyses*

The emission analysis focuses on evaluating the environmental impact of various energy sources, emphasizing the importance of selecting preferred energy options based on their emissions. This study specifically examines the role of renewable energy (RE), particularly solar power, in mitigating CO2 emissions. The impact of various energy sources on the environment is highlighted as a crucial factor in determining the preferred energy source. Utilizing RE, such as solar power, to meet energy requirements is viewed as an effective method for reducing $CO_2$ emissions. In this study, the annual mitigation of $CO_2$ and the calculation of carbon credits for the solar ORC system were explored [43]:

$$\varphi_{CO_2} = \frac{\psi_{CO_2} \times E_{en,ann}}{10^3} \quad (16)$$

Where: $\varphi_{CO_2}$ (ton) represents the annual $CO_2$ emissions − $\psi_{CO_2}$ (kg$CO_2$/kWh) denotes the average $CO_2$ emissions from coal power production, set at 2.04 − $E_{en,ann}$ (kWh) indicates the electricity generated by the solar or ORC systems over a year (2500 h for Tehran, Iran). Also, carbon credit $Z_{CO_2}$ is calculated using Eq. **(17)** with $z_{CO_2}$ set at \$14.5 per ton − $\varphi_{CO_2}$ (ton) signifies the annual $CO_2$ emissions [43]:

$$Z_{CO_2} = z_{CO_2} \times \varphi_{CO_2} \quad (17)$$

These analyses offer a clear framework for understanding how the adoption of solar energy through the ORC system not only contributes to emission reductions but also creates potential financial benefits through carbon credits.

*Case study*

In this study, the 16 counties in Tehran province, Iran, were evaluated. The city of Tehran is located at 51° 6′ to 51° 38′ east longitude and 35° 34′ to 35° 51′ north latitude and its height from the open water level is between 1800 m in the north and 1200 m in the center, and 1050 m in the south is variable. Tehran is spread between two valleys of mountains and deserts and on the southern slopes of the Alborz mountain range. Fig. 3a presents a view of the selected area for research. On the other hand, the variation of daily radiation from 2001 to 2022 for Tehran, Iran is presented in Fig. 3b. The analysis covers the period from 2001 to 2022, allowing for a comprehensive evaluation of trends and developments over a significant duration. This extensive timeframe is essential for capturing long-term patterns, assessing the impact of technological advancements, and understanding the effects of policy changes on energy systems. By including a 21-year span, the study can provide insights into both gradual shifts and abrupt changes within the field, facilitating a more robust and informed analysis. It should be mentioned that these data were used for optical and thermal analyses of the solar ORC system.

It is important to note that this study calculated and reported various energy parameters, including cavity heat gain, cavity heat losses, and thermal efficiency. Additionally, it assessed several exergy parameters such as exergy losses and exergy efficiency. Furthermore, the study examined factors related to the development of a solar Organic Rankine Cycle (ORC) system with both vacuum and non-vacuum cavity receivers. This included calculations of the annual power generated by a single ORC unit, the total number of ORC systems required, and the land area necessary to supply 10 % of the power demand in Tehran's industrial sector in 2022.

The results of the current system was validated based on the reported results by Ref. [44]. A cylindrical cavity receiver with aperture diameter of 10.2 cm, and 15.2 cm were investigated in Ref. [44]. Fig. 3c presents a comparison of our modeling results with the experimental data from [44] regarding the cylindrical cavity. There is a strong correlation between our findings and the experimentally reported results from [44].


**(a)**

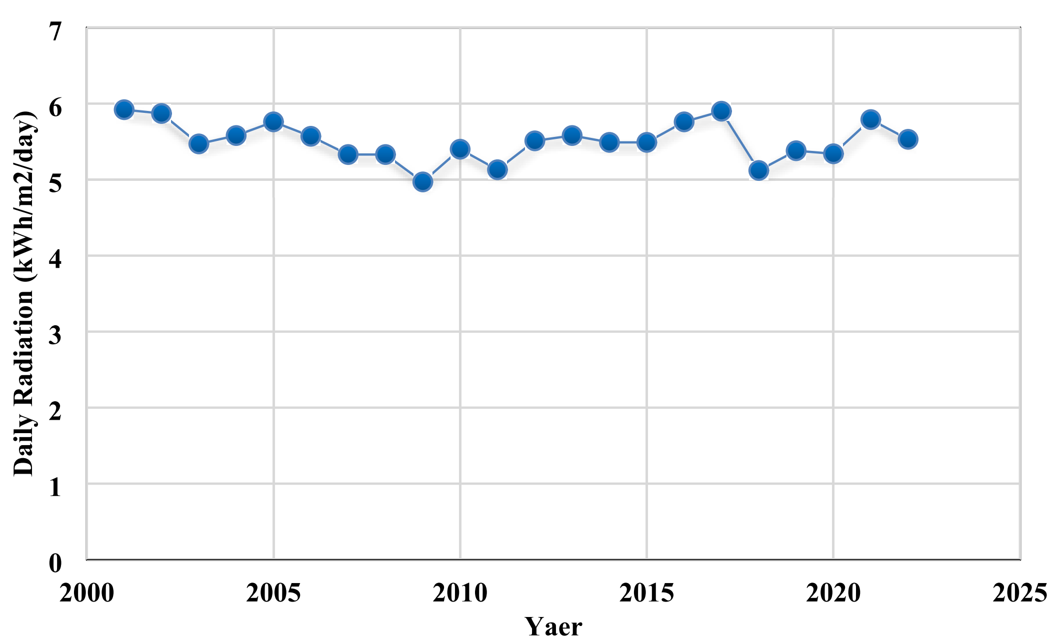


**(b)**

**Fig. 3.** View of a) Iran, Tehran Mape, (https://www.google.com/maps/), b) variation of daily radiation from 2001 to 2022 for Tehran, Iran (https://www.nasa.gov/), and Comparison between reported results by Ref. [44] and current research.

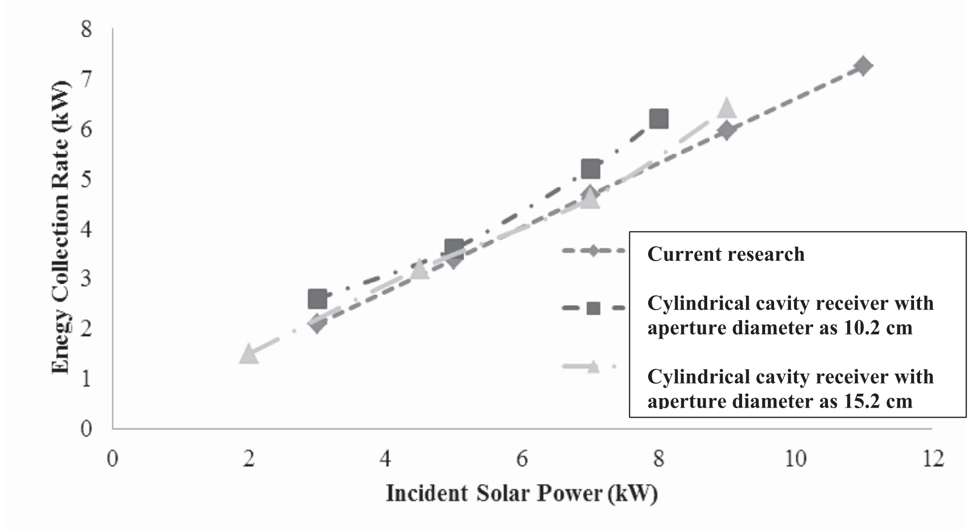


**(c)**

**Fig. 3.** (*continued*).

## Result and Discussion

*Solar power plant*

Fig. 4a presents variations of heat gained and solar radiation in different years from 2001 to 2022, using vacuum and non-vacuum cylindrical CRs for Tehran, Iran. Thermal oil was used as the solar working fluid. The vacuum and non-vacuum cylindrical CRs had an aperture diameter of 0.14 m, height of 0.14 m, and diameter tube of 0.01 m. The solar working fluid was entered into the CRs with a temperature of 100 °C, and mass flow rate of 0.04 kg/s. Also, the optical efficiency of the solar system was calculated as 0.93, and solar radiation was assumed based on the reported data in Fig. 3b. As reported in Fig. 4a, the solar system with the vacuum CR resulted in a higher amount of heat gained compared to the non-vacuum one. This matter is due to the higher amount of cavity heat losses of the non-vacuum CR compared to the vacuum one, as shown in Fig. 4b.

It is important to acknowledge that there were certain limitations in modeling and analyzing the system, particularly regarding the assumed solar radiation data. The solar radiation data were based on an annual average derived from reports provided by NASA (https://www.nasa.gov/).

Variation of heat losses, and solar radiation via different years from 2001 to 2022 using vacuum and non-vacuum cylindrical CRs for Tehran, Iran, are shown in Fig. 4b. The solar working fluid was Thermal oil. The structure dimensions of the vacuum and non-vacuum cylindrical CRs included aperture diameter of 0.14 m, height of 0.14 m, and diameter tube of 0.01 m. Thermal oil was entered into the CRs with a temperature of 100 °C with a mass flow rate of 0.04 kg/s. The solar system's optical efficiency was 0.93. As mentioned in the previous paragraph, the non-vacuum CR resulted in higher heat losses compared to the vacuum one due to higher convection heat losses in the non-vacuum CR.

Fig. 4c depicts variation in thermal efficiency and solar radiation in different years from 2001 to 2022, using the vacuum and non-vacuum cylindrical CRs in Tehran, Iran. As mentioned, Thermal oil was used as the solar working fluid. The vacuum and non-vacuum cylindrical CRs had an aperture diameter of 0.14 m, a cavity height of 0.14 m, and a diameter tube of 0.01 m. The inlet temperature and the mass flow rate of the solar working fluid were 100 °C, and 0.04 kg/s, respectively. The solar radiation was used based on the reported data in Fig. 4c, and the optical efficiency of the solar system was calculated as 0.93. It can be seen that the solar system with the vacuum cylindrical CR resulted in a higher amount of thermal efficiency compared to the non-vacuum one. This issue is due to higher values of the heat gained, and lower amounts of heat losses of the vacuum CR compared to the non-vacuum one, as presented in Fig. 4a, and Fig. 4b, respectively. Also, it can be seen that the thermal efficiency of the solar system with the vacuum, and non-vacuum CR were reported at about 0.765 %, and 0.66 %, respectively.

Variation of Exergy losses of the solar system via different years from 2001 to 2022 using vacuum and non-vacuum cylindrical CRs for Tehran, Iran, are presented in Fig. 5a. As mentioned, thermal oil was used as the solar working fluid with the inlet temperature of 100 °C and the mass flow rate of 0.04 kg/s. The vacuum and non-vacuum cylindrical CRs were used with an aperture diameter of 0.14 m, cavity height of 0.14 m, and diameter tube of 0.01 m. The Solar radiation from 2001 up to 2022 was used based on the presented data in Fig. 3b. The optical efficiency of the solar system was assumed to be 0.93 based on the optical analysis. It can be concluded from Fig. 5a, that the solar system with the non-vacuum CR resulted in higher Exergy losses compared to the solar system with the vacuum CR. Also, it can be seen that data on the Exergy losses for both the examined CRs had similar fluctuations, such as variations in solar radiation from 2001 to 2022.

Fig. 5b shows the variation of Exergy efficiency of the solar system using vacuum and non-vacuum cylindrical CRs via different years from 2001 to 2022 for Tehran, Iran. Thermal oil with an inlet temperature of 100 °C and a mass flow rate of 0.04 kg/s was used as the solar working fluid. Structure dimensions of the vacuum and non-vacuum cylindrical CRs included an aperture diameter of 0.14 m, a cavity height of 0.14 m, and a tube diameter of 0.01 m. The optical efficiency of the solar system based on the optical analysis was equal to 0.93, and the variation of the solar radiation was presented in Fig. 3b. It can be seen, that the solar system with the vacuum CR resulted in higher amounts of the Exergy efficiency compared to the solar system with the non-vacuum one. This issue is due to higher values of the Exergy losses of the solar system with the non-vacuum CR than the solar system with the vacuum CR. Also, the data analysis reveals that both CRs exhibited comparable fluctuations in Exergy efficiency, mirroring the variations in solar radiation from 2001 to 2022.

Power generation by one unit of the solar ORC system using vacuum and non-vacuum CRs from 2001 to 2022 is reported in Table 1. The solar dish concentrator with the vacuum and non-vacuum CRs was used as the heat source of the ORC system. Propene was used as the ORC working fluid with a constant turbine inlet pressure of 3 MPa. Also, the condenser temperature was assumed as a constant amount of 38 °C during the solar

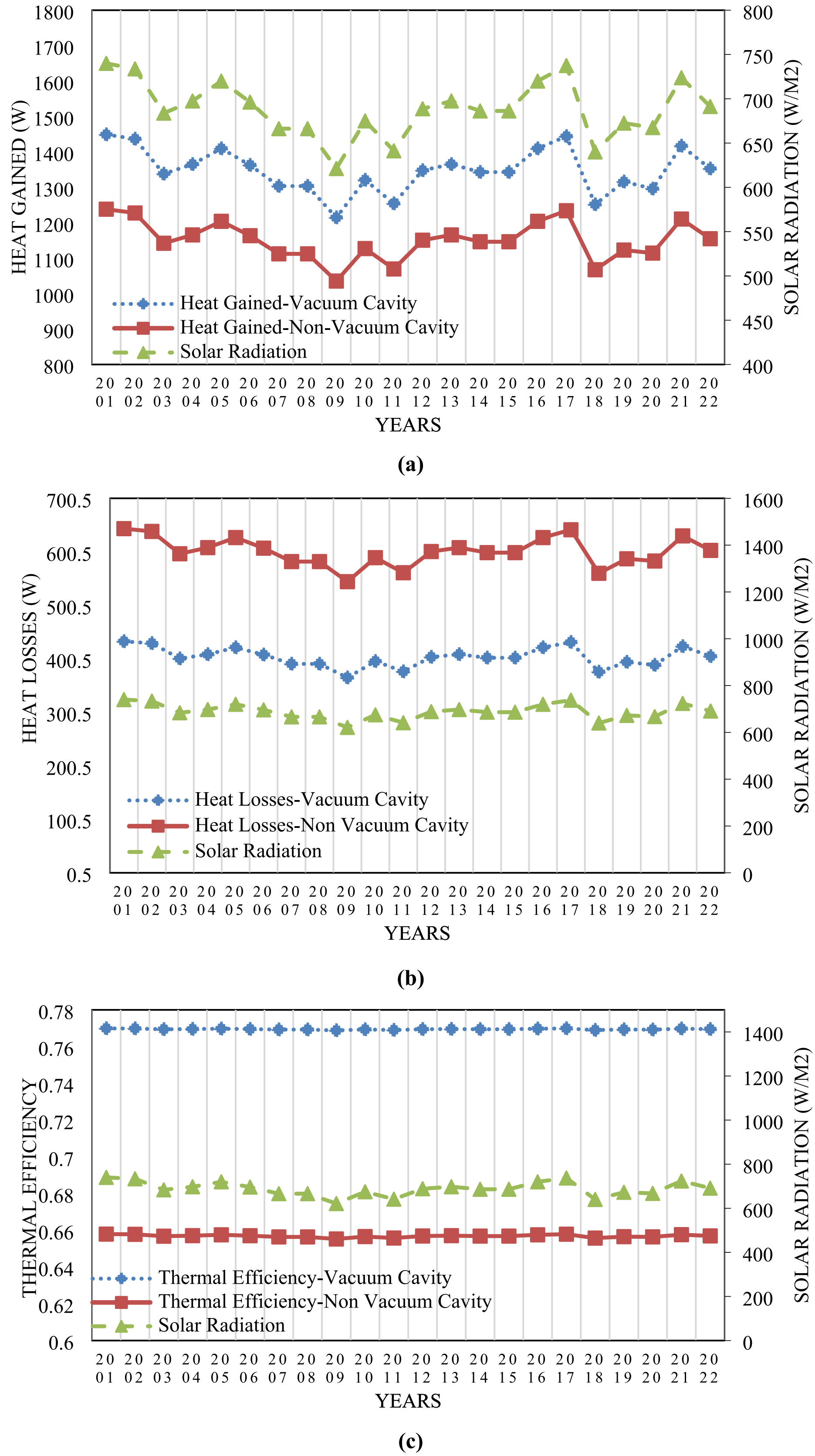


**Fig. 4.** Variation of a) heat gained, and solar radiation, b) heat losses, and solar radiation, and c) thermal efficiency, and solar radiation via different years from 2001 to 2022 using vacuum and non-vacuum cylindrical CRs.

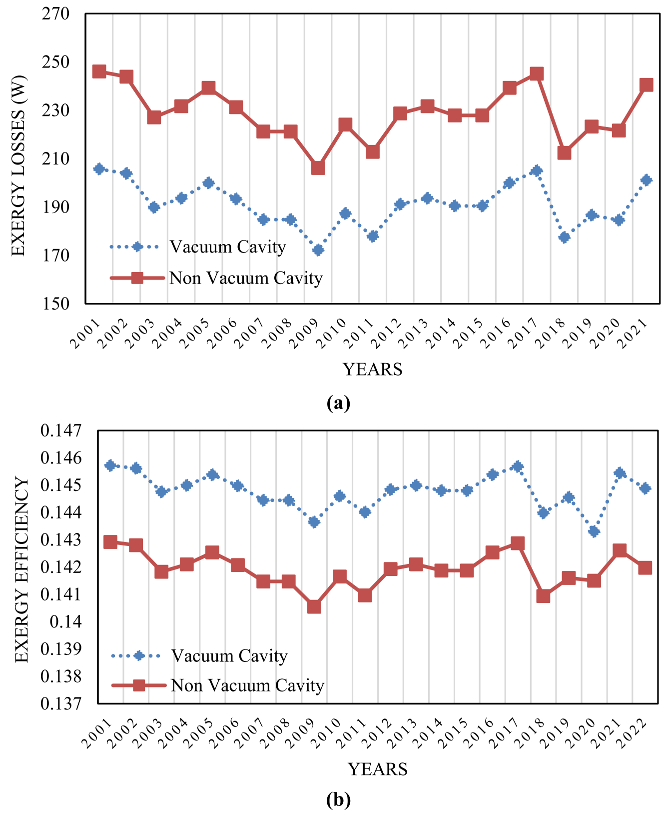


**Fig. 5.** Variation of a) Exergy losses, and b) Exergy efficiency via different years from 2001 to 2022 using vacuum and non-vacuum cylindrical CRs.

ORC system analyses. In the same condition, the solar ORC system with the vacuum CR generated a higher amount of yearly power generation than the solar ORC system with the non-vacuum CR. This issue is due to the better energy and Exercise performance of the solar system with the vacuum CR than the non-vacuum one, as discussed in the previous paragraphs.

Table 1 reports the required land to provide 10 % of the required power in the industrial sector of Tehran, Iran, by the solar ORC system in 2022. It should be mentioned that the solar dish concentrator with the vacuum and non-vacuum CRs was used as the heat source of the ORC system. The ORC working fluid was Propene with a constant turbine inlet pressure of 3 MPa. Also, the ORC system was analyzed with a constant condenser temperature of 38 °C. It can result from Table 1 that the required land for providing 10 % of the yearly required power in the industrial sector of Tehran in 2022 was about 459 ha and 538 ha using the vacuum, and non-vacuum CR as the heat source of the solar ORC system, respectively. Also, the land required to provide 10 % of the annual electricity requirement in the industrial sector of different cities of Tehran province in 2022 is presented separately in Table 1. This table indicates the number of solar ORC systems needed to provide 10 % of the annual electricity for the industrial sector across various cities in Tehran, Iran. Additionally, the "Required Land (ha)" column shows the land necessary for installing the solar ORC systems, based on the assumption that each setup requires 8 m$^2$ of space.

*Emission reduction*

Table 2 reports yearly amounts of the carbon mitigated (ton$Co_2$) and carbon credits ($) using the application of one unit of the solar ORC system using vacuum and non-vacuum CR from 2001 to 2022. It can be seen that the solar ORC system using the vacuum CR resulted in higher values of the carbon mitigated (ton$Co_2$) and carbon credits ($) compared to the application of the non-vacuum CR during a year. In other words, the suggested ORC system using the vacuum CR is a more effective solution for reducing $CO_2$ emissions and improving environmental conditions.

Table 3 presents amounts of carbon mitigated (ton $Co_2$) and carbon credits ($) using the development of the suggested solar ORC system to provide 10 % of the required power in the industrial sector of Tehran, Iran, in 2022. It can be concluded from Table 3 that the development of the suggested solar ORC system can result in a carbon mitigation of 1676641.50 (tons of $CO_2$) and carbon credits of 24311287.31 ($), which are significant values for effective environmental impact and the development of good energy governance.

*Governance policy*

Policy development involves the translation of governmental political objectives into strategies and measures to achieve specific outcomes. Public policy matters are intricate, emerging in dynamic and uncertain settings characterized by conflicting interests. A policy comprises defined and purposeful actions individuals or groups undertake to tackle an issue or challenge. It is the governmental choices that establish objectives and identify methods for attainment. Typically, public policy research categorizes policymaking into three phases: policy design and enactment, policy execution, and policy assessment.

Energy policy encompasses a set of formal and informal guidelines and strategies that evolve over many years. The formulation of energy policies involves fundamental considerations related to energy

**Table 1**
Required land for providing 10% of the required power in the industrial sector of Tehran, Iran, by the solar ORC system in 2022.

| Cities | 10 % of Industrial Sector (Yearly-MWh) | Power Generation by one unit (Yearly-MWh) | | Solar ORC Number | | Required Land (ha) | |
|---|---|---|---|---|---|---|---|
| | | Vacuum | Non Vacuum | Vacuum | Non Vacuum | Vacuum | Non Vacuum |
| EslamShahr | 53777.20 | 1.43 | 1.22 | 37,535 | 43,964 | 30.03 | 35.17 |
| Baharestan | 10648.20 | 1.43 | 1.22 | 7432 | 8705 | 5.95 | 6.96 |
| Pakdasht | 86412.80 | 1.43 | 1.22 | 60,313 | 70,645 | 48.25 | 56.52 |
| Pardis | 28393.00 | 1.43 | 1.22 | 19,817 | 23,212 | 15.85 | 18.57 |
| Pishva | 2707.20 | 1.43 | 1.22 | 1890 | 2213 | 1.51 | 1.77 |
| Tehran | 214769.80 | 1.43 | 1.22 | 149,903 | 175,581 | 119.92 | 140.46 |
| Damavand | 5545.60 | 1.43 | 1.22 | 3871 | 4534 | 3.10 | 3.63 |
| RobatKarim | 48554.80 | 1.43 | 1.22 | 33,890 | 39,695 | 27.11 | 31.76 |
| Ray | 191992.40 | 1.43 | 1.22 | 134,005 | 156,959 | 107.20 | 125.57 |
| Shemiranat | 743.50 | 1.43 | 1.22 | 519 | 608 | 0.42 | 0.49 |
| Shahryar | 43472.70 | 1.43 | 1.22 | 30,343 | 35,540 | 24.27 | 28.43 |
| Firozkoh | 24661.20 | 1.43 | 1.22 | 17,213 | 20,161 | 13.77 | 16.13 |
| Ghods | 43079.70 | 1.43 | 1.22 | 30,068 | 35,219 | 24.05 | 28.18 |
| Gharchak | 14424.20 | 1.43 | 1.22 | 10,068 | 11,792 | 8.05 | 9.43 |
| Malard | 29370.30 | 1.43 | 1.22 | 20,500 | 24,011 | 16.40 | 19.21 |
| Varamin | 23330.00 | 1.43 | 1.22 | 16,284 | 19,073 | 13.03 | 15.26 |
| Summation | | | | | | 458.92 | 537.53 |

**Table 2**
Amounts of carbon mitigated ($tonco_2$) and carbon credits ($) using the development of one unit of the solar ORC system using vacuum and non-vacuum CR from 2001 to 2022.

| | Generated power (kW.h) | | Vacuum | | Non Vacuum | |
|---|---|---|---|---|---|---|
| Years | Vacuum | Not Vacuum | $\varphi$($tonco_2$) | *Zeth*($) | $\varphi$($tonco_2$) | Zeth ($) |
| 2001 | 1560.21 | 1333.33 | 3.18 | 46.15 | 2.72 | 39.44 |
| 2002 | 1546.94 | 1321.83 | 3.16 | 45.76 | 2.70 | 39.10 |
| 2003 | 1440.74 | 1229.84 | 2.94 | 42.62 | 2.51 | 36.38 |
| 2004 | 1469.94 | 1255.14 | 3.00 | 43.48 | 2.56 | 37.13 |
| 2005 | 1517.73 | 1296.53 | 3.10 | 44.89 | 2.64 | 38.35 |
| 2006 | 1467.29 | 1252.84 | 2.99 | 43.40 | 2.56 | 37.06 |
| 2007 | 1403.57 | 1197.64 | 2.86 | 41.52 | 2.44 | 35.43 |
| 2008 | 1403.57 | 1197.64 | 2.86 | 41.52 | 2.44 | 35.43 |
| 2009 | 1307.99 | 1114.85 | 2.67 | 38.69 | 2.27 | 32.98 |
| 2010 | 1422.16 | 1213.74 | 2.90 | 42.07 | 2.48 | 35.90 |
| 2011 | 1350.47 | 1151.65 | 2.75 | 39.95 | 2.35 | 34.07 |
| 2012 | 1451.36 | 1239.04 | 2.96 | 42.93 | 2.53 | 36.65 |
| 2013 | 1467.41 | 1252.97 | 2.99 | 43.41 | 2.56 | 37.06 |
| 2014 | 1441.10 | 1230.21 | 2.94 | 42.63 | 2.51 | 36.39 |
| 2015 | 1438.66 | 1228.13 | 2.93 | 42.56 | 2.51 | 36.33 |
| 2016 | 1507.44 | 1287.74 | 3.08 | 44.59 | 2.63 | 38.09 |
| 2017 | 1541.79 | 1317.52 | 3.15 | 45.61 | 2.69 | 38.97 |
| 2018 | 1334.25 | 1137.78 | 2.72 | 39.47 | 2.32 | 33.66 |
| 2019 | 1400.29 | 1195.01 | 2.86 | 41.42 | 2.44 | 35.35 |
| 2020 | 1377.07 | 1184.00 | 2.81 | 40.73 | 2.42 | 35.02 |
| 2021 | 1503.02 | 1284.05 | 3.07 | 44.46 | 2.62 | 37.98 |
| 2022 | 1432.73 | 1223.20 | 2.92 | 42.38 | 2.50 | 36.18 |
| Sum | | | 64.84 | 940.22 | 55.38 | 802.94 |

**Table 3**
Amounts of carbon mitigated ($tonco_2$) and carbon credits ($) using the development of the solar ORC system for providing 10% of the required power in the industrial sector of Tehran, Iran, in 2022.

| Cities | 10 % of Industrial (Yearly-MWh) | $\varphi$($tonco_2$) | Zeth ($) |
|---|---|---|---|
| EslamShahr | 53777.20 | 109705.49 | 1590729.58 |
| Baharestan | 10648.20 | 21722.33 | 314973.76 |
| Pakdasht | 86412.80 | 176282.11 | 2556090.62 |
| Pardis | 28393.00 | 57921.72 | 839864.94 |
| Pishva | 2707.20 | 5522.69 | 80078.98 |
| Tehran | 214769.80 | 438130.39 | 6352890.68 |
| Damavand | 5545.60 | 11313.02 | 164038.85 |
| RobatKarim | 48554.80 | 99051.79 | 1436250.98 |
| Ray | 191992.40 | 391664.50 | 5679135.19 |
| Shemiranat | 743.50 | 1516.74 | 21992.73 |
| Shahryar | 43472.70 | 88684.31 | 1285922.47 |
| Firozkoh | 24661.20 | 50308.85 | 729478.30 |
| Ghods | 43079.70 | 87882.59 | 1274297.53 |
| Gharchak | 14424.20 | 29425.37 | 426667.84 |
| Malard | 29370.30 | 59915.41 | 868773.47 |
| Varamin | 23330.00 | 47593.20 | 690101.40 |
| Sum | | 1676640.50 | 24311287.31 |

generation and utilization, influencing economic growth, sustainability, and societal acceptance. Energy policy development emphasizes sustainable energy strategies and transitioning to a low-carbon economy by reducing reliance on fossil fuels, promoting RE sources, enhancing energy efficiency, and advancing towards a smart grid system. Determining the optimal mix of energy sources for each nation to maximize efficiency has been a key focus. This concept is encapsulated in the notion of an "Energy Basket," which serves as the core of a country's energy planning, consisting of various primary energy sources used to generate secondary energy for direct consumption.

The energy mix of any country is determined by the availability of resources within its borders or the potential for importing them. Policies for developing RE encompass all strategies aimed at achieving specific targets for various RE sources. An effective RE policy should consider local conditions and be tailored to the unique political, economic, and social dynamics of each region or country where it will be implemented. Support measures for RE have been extensively implemented across electricity generation, heating/cooling, and transportation sectors. Current trends in RE policy focus on integrating policy tools, establishing linkages among electricity, heating/cooling, and transportation policies, and creating innovative mechanisms to enhance the integration of RE sources into energy systems.

The foundation for advancing RE lies in the availability of sufficient RE resources. Pursuing RE development without adequate potential is ultimately futile and unproductive. Many governments extensively utilize resource estimates and potentials to inform policy and planning processes. RE targets have become a prevalent tool for ensuring a secure and sustainable energy future. These targets are instrumental in shaping both national and global energy landscapes, offering a roadmap for RE trends and facilitating the realization of medium and long-term aspirations. As of the end of 2016, a minimum of 176 countries had established RE goals. Among them, at least 150 countries had set targets concerning the RE share in electricity generation, 47 countries had specific goals for renewable heating/cooling, and 41 countries had targets for RE use in transportation. To be effective, these targets necessitate the implementation of cross-sectoral policies and coordinated actions encompassing the heating/cooling, transportation, and electricity sectors.

The International Energy Agency defines RE as "energy derived from natural processes that are sustainable, repeatable, and sourced from the sun or heat generated from within the earth." Energy generated from solar, wind, biomass, geothermal, hydropower, ocean, biofuels, and hydrogen sourced from renewable origins falls under the category of renewable energies (IEA, 2012). The advancement of RE is a key strategic policy for countries to meet energy demands, address environmental concerns, and combat climate change challenges. Three primary drivers fueling the growth of RE technologies in recent years include rising energy demands, the finite nature of fossil fuels, and the urgency of climate change mitigation. Consequently, the three core objectives of RE policy, referred to as the "magic triangle" of RE policy objectives, encompass energy security, sustainability/environmental protection, and economic development (Korte-Jordan, 2011). In addition to these objectives, the development of RE brings about various other benefits and necessities, such as fostering technological innovation, poverty reduction, decreasing reliance on fossil fuels, water and land conservation, infrastructure development, job creation, and enhancing national security.

At the 2012 United Nations Conference on Sustainable Development, member countries collectively established sustainable development goals (SDGs), and in 2015, the United Nations General Assembly set forth 17 goals to be achieved by 2030. Additionally, in December 2015, during the 21st annual meeting following the 1992 United Nations Conference on Environment and Development (UNCED), the Paris Agreement was ratified. Regarded as a pivotal moment in addressing climate change, this agreement signifies a commitment by its signatories to combat global warming by limiting the temperature increase to 2 degrees Celsius, with a preference for a 1.5-degree target above pre-industrial levels. In 2021, at the 26th annual meeting, members adopted the Glasgow Climate Accord, which includes provisions to enhance climate resilience, reduce greenhouse gas emissions, and ensure that developed countries contribute $100 billion annually to support climate actions in developing nations. Furthermore, countries are urged to phase out inefficient fossil fuel subsidies as part of their climate mitigation efforts.

Prioritizing RE sources is crucial for reducing $CO_2$ and other greenhouse gas emissions, safeguarding environmental quality, ensuring stable or sustainable energy supplies, and advancing on the path of sustainable development. The seventh objective of the 2030 sustainable development agenda aims to provide universal access to affordable, reliable, sustainable, and modern energy. While the utilization of RE has grown in recent years, the 2020 United Nations report highlights that the proportion of RE in total final energy consumption rose from 16.3 percent in 2010 to 17.3 percent in 2017. However, achieving long-term climate targets will necessitate further advancements in this regard.

Government policies are pivotal in driving investments and accelerating the adoption of RE technologies. A crucial aspect of designing effective RE targets involves aligning these targets with specific policies or actions for implementation. Establishing RE targets marks the initial step in shaping precise policies, support mechanisms, incentives, or investment frameworks that empower market participants to meet these targets efficiently. These policies serve to mitigate risks, promote RE utilization and are typically integrated within a comprehensive policy framework. When a country sets its RE objectives and crafts corresponding strategies and policies, ensuring the stability and security of planning is paramount. Policy instruments serve as essential mechanisms for attaining key objectives, acting as governance tools or methodologies to tackle challenges effectively. A combination of policy measures emphasizing direct support for RE deployment, integration, and fostering an enabling environment is essential. Most analyses of RE tools focus on enhancing the RE market and reducing production costs. It is crucial to recognize that the successful implementation of policy tools to increase the penetration of clean technologies in energy markets hinges on a comprehensive understanding of their effective deployment. Broadly, RE policy tools can be categorized into three main groups: financial incentives, binding regulations and mechanisms, and complementary measures. Drawing from this research, adopting a solar Organic Rankine Cycle (ORC) system utilizing a vacuum cylindrical CR could be recommended as a promising approach to curbing $CO_2$ emissions in Tehran, Iran. Enhancing energy governance can be achieved by applying and developing the suggested solar ORC system in Iran.

## Conclusions

Given the detrimental effects of non-renewable energy sources on the environment and their finite availability, shifting towards renewable energy (RE) is essential for global conservation. Renewable energy plays a vital role in reducing air pollution and greenhouse gas emissions, while also decreasing dependence on oil, thus enhancing environmental sustainability. This study explores the implementation of a solar Organic Rankine Cycle (ORC) system with an innovative vacuum cylindrical condenser design for power generation. Optical and thermal evaluations of this system were conducted in Tehran, Iran, between 2001 and 2022. The research also examines the potential for emission reductions and land requirements linked to the deployment of the solar ORC system. Furthermore, discussions focus on enhancing energy governance through the development of these recommended power plant systems. The key findings of the study are as follows:

- The solar system equipped with the vacuum cylindrical receiver (CR) exhibited greater heat gain and thermal efficiency than the non-vacuum system, due to reduced heat losses in the vacuum receiver. The thermal efficiencies for the solar systems were approximately 76.5 % for the vacuum CR and 66 % for the non-vacuum CR.
- The non-vacuum CR system showed higher exergy losses and lower exergy efficiency compared to its vacuum counterpart. Both types of CR demonstrated similar variations in energy and exergy performance, mirroring changes in solar radiation from 2001 to 2022. Also, the solar ORC system with the vacuum CR produced more annual power than the non-vacuum system.
- To meet 10 % of Tehran's industrial power demand in 2022, approximately 459 ha of land were required for the vacuum CR, compared to 538 ha for the non-vacuum CR within the solar ORC system.
- The ORC system utilizing the vacuum CR emerged as a more effective solution for reducing $CO_2$ emissions and enhancing environmental quality, leading to significant carbon mitigation and generation of carbon credits. The implementation of the proposed solar ORC system has the potential to achieve carbon mitigation of 1,676,641.50 tons of $CO_2$ and generate carbon credits valued at $24,311,287.31. These figures represent substantial contributions to positive environmental impact and the advancement of effective energy governance.
- Finally, the proposed solar ORC system offers considerable environmental advantages and supports the development of effective energy governance.

Developing a dynamic model for the solar ORC system is suggested for the future works that can help researchers and engineers better understand how the system operates under a variety of conditions. This understanding is crucial for optimizing design choices, improving efficiency, and integrating the system more effectively into broader energy solutions. Ultimately, it could lead to more reliable and commercially viable solar ORC systems. Future works could include:

- Improving system design based on insights gained from dynamic simulations.
- Optimizing control strategies to maximize performance based on real-time data.
- Conducting real-time monitoring and adjustments based on dynamic modeling outcomes.

## CRediT authorship contribution statement

**Reyhaneh Loni:** Writing – original draft, Software, Methodology, Formal analysis, Data curation. **Alibakhsh Kasaeian:** Writing – review & editing, Resources, Project administration, Methodology. **Mohsen Sharifpur:** Writing – review & editing, Visualization, Project administration, Data curation, Conceptualization. **Gholamhassan Najafi:** Writing – review & editing, Methodology, Conceptualization.

## Declaration of competing interest

The authors declare that they have no known competing financial interests or personal relationships that could have appeared to influence the work reported in this paper.

## Data availability

Data will be made available on request.

## References

[1] Somoye OA. Energy crisis and renewable energy potentials in Nigeria: A review. Renew Sustain Energy Rev 2023;188:113794.
[2] Chi Y, Esily RR, Ibrahiem DM, Houssam N, Chen Y, Jia X, et al. Is North Africa region on track to energy trilemma for enhancing economic progress? The role of population growth and energy usage, Energy Strategy Reviews 2023;50:101245.
[3] Pan Y, Zhang C-C, Lee C-C, Lv S. Environmental performance evaluation of electric enterprises during a power crisis: Evidence from DEA methods and AI prediction algorithms. Energy Econ 2024;130:107285.
[4] Majeed Y, Khan MU, Waseem M, Zahid U, Mahmood F, Majeed F, et al. Renewable energy as an alternative source for energy management in agriculture. Energy Rep 2023;10:344–59.
[5] Paraschiv S. Analysis of the variability of low-carbon energy sources, nuclear technology and renewable energy sources, in meeting electricity demand. Energy Rep 2023;9:276–83.
[6] Keshuov S, Moldybayeva N. Selection of optimal structure of an energy-supply system for objects in an agro-industrial complex based on renewable-energy sources. Renewable Energy Focus 2024;48:100533.
[7] Shahverdi K, Najafi G, Mamat R, Ghazali MF, Ei-Shafy A, Mousa M. Introducing a design procedure for Archimedes Screw Turbine based on optimization algorithm. Energy Sustain Dev 2023;72:162–72.
[8] Zambrano-Monserrate MA. Clean energy production index and CO2 emissions in OECD countries. Sci Total Environ 2024;907:167852.
[9] Bergougui B. Moving toward environmental mitigation in Algeria: Asymmetric impact of fossil fuel energy, renewable energy and technological innovation on CO2 emissions. Energ Strat Rev 2024;51:101281.
[10] Hoseinzadeh S, Groppi D, Nastasi B, Bruschi D, Garcia DA. Designing high-share 50% and 100% renewable energy scenarios for Ragusa by sustainable energy toolkit application. Sustainable Energy Technol Assess 2024;63:103645.
[11] Pourasl HH, Barenji RV, Khojastehnezhad VM. Solar energy status in the world: A comprehensive review. Energy Rep 2023;10:3474–93.

[12] Falope T, Lao L, Hanak D, Huo D. Hybrid energy system integration and management for solar energy: A review. Energy Conversion and Management: X 2024;100527.

[13] Lima GM, Belchior FN, Villena JEN, Domingos JL, Freitas MAV, Hunt JD. Hybrid electrical energy generation from hydropower, solar photovoltaic and hydrogen. Int J Hydrogen Energy 2024;53:602–12.

[14] Ilham NI, Dahlan NY, Hussin MZ. Optimizing solar PV investments: A comprehensive decision-making index using CRITIC and TOPSIS. Renewable Energy Focus 2024;100551.

[15] Carro A, Chacartegui R, Ortiz C, Becerra J. Indirect power cycles integration in concentrated solar power plants with thermochemical energy storage based on calcium hydroxide technology. J Clean Prod 2023;421:138417.

[16] Hadidi A. Thermodynamic design of the novel energy storage system based on liquid carbon dioxide for a 17 MW concentrated solar thermal power plant. J Storage Mater 2024;83:110761.

[17] Loni R, Kasaeian A, Mahian O, Sahin A. Thermodynamic analysis of an organic rankine cycle using a tubular solar cavity receiver. Energ Conver Manage 2016; 127:494–503.

[18] Rahmdel M, Behzadmehr A, Sadeghi J, Farzaneh H, Sarhaddi F. Conceptual design of an innovative flexible and controllable Solar ORC cogeneration system for operating in remote areas. Sol Energy 2023;262:111899.

[19] Motlagh SHB, Hosseini SA, Pons-Valladares O. Integrated value model for sustainability assessment of residential solar energy systems towards minimizing urban air pollution in Tehran. Sol Energy 2023;249:40–66.

[20] Liu Y, Ming T, Peng C, Wu Y, Li W, De Richter R, et al. Mitigating air pollution strategies based on solar chimneys. Sol Energy 2021;218:11–27.

[21] Hachicha AA, Abo-Zahhad EM, Oh S, Issa S, Rahman S. Numerical investigation and optimization of a novel hybrid solar chimney for air pollution mitigation and clean electricity generation. Appl Therm Eng 2023;226:120271.

[22] Manrique JA, Villaseñor JM. Air pollution dispersion by using solar energy. Int Commun Heat Mass Transfer 1994;21:29–39.

[23] Yang L, Gao X, Li Z, Jia D. Quantitative effects of air pollution on regional daily global and diffuse solar radiation under clear sky conditions. Energy Rep 2022;8: 1935–48.

[24] Rafiei A, Loni R, Mahadzir SB, Najafi G, Sadeghzadeh M, Mazlan M, et al. Hybrid solar desalination system for generation electricity and freshwater with nanofluid application: Energy, exergy, and environmental aspects. Sustainable Energy Technol Assess 2022;50:101716.

[25] Loni R, Kasaeian A, Asli-Ardeh EA, Ghobadian B. Optimizing the efficiency of a solar receiver with tubular cylindrical cavity for a solar-powered organic Rankine cycle. Energy 2016;112:1259–72.

[26] R.a. Loni, E.A. Asli-Ardeh, B. Ghobadian, A. Kasaeian, S. Gorjian, Thermodynamic analysis of a solar dish receiver using different nanofluids, Energy, 133 (2017) 749-760.

[27] Morid M, Manesh MHK. 6E evaluation of an innovative polygeneration system consisting of gas turbine cycle with CO2 capture, ejector refrigeration cycle, steam Rankine cycle, solar tower and MEDAD unit. Thermal science and Engineering progress 2023;46:102234.

[28] Ghorbani B, Ebrahimi A, Moradi M. Exergy, pinch, and reliability analyses of an innovative hybrid system consisting of solar flat plate collectors, Rankine/CO2/ Kalina power cycles, and multi-effect desalination system. Process Saf Environ Prot 2021;156:160–83.

[29] Mei B, Qin Y, Taghavi M. Thermodynamic performance of a new hybrid system based on concentrating solar system, molten carbonate fuel cell and organic Rankine cycle with CO2 capturing analysis. Process Saf Environ Prot 2021;146: 531–51.

[30] Fan G, Song J, Zhang J, Fu Z, Gong X, Dai Y, et al. Thermo-economic assessment and systematic comparison of combined supercritical CO2 and organic Rankine cycle (SCO2-ORC) systems for solar power tower plants. Appl Therm Eng 2024; 236:121715.

[31] Shahverdi K, Loni R, Ghobadian B, Monem M, Gohari S, Marofi S, et al. Energy harvesting using solar ORC system and Archimedes Screw Turbine (AST) combination with different refrigerant working fluids. Energ Conver Manage 2019; 187:205–20.

[32] Refiei A, Loni R, Najafi G, Sahin A, Bellos E. Effect of use of MWCNT/oil nanofluid on the performance of solar organic Rankine cycle. Energy Rep 2020;6:782–94.

[33] Loni R, Mahian O, Markides CN, Bellos E, Le Roux WG, Kasaeian A, et al. A review of solar-driven organic Rankine cycles: Recent challenges and future outlook. Renew Sustain Energy Rev 2021;150:111410.

[34] Shahverdi K, Bellos E, Loni R, Najafi G, Said Z. Solar-driven water pump with organic Rankine cycle for pressurized irrigation systems: A case study. Thermal Science and Engineering Progress 2021;25:100960.

[35] Loni R, Kasaeian A, Asli-Ardeh EA, Ghobadian B, Le Roux W. Performance study of a solar-assisted organic Rankine cycle using a dish-mounted rectangular-cavity tubular solar receiver. Appl Therm Eng 2016;108:1298–309.

[36] Ardeh E-A-A, Loni R, Najafi G, Ghobadian B, Bellos E, Wen D. Exergy and economic assessments of solar organic Rankine cycle system with linear V-Shape cavity. Energ Conver Manage 2019;199:111997.

[37] Bode S-J, Gauché P. Review of optical software for use in concentrating solar power systems. 1st South African Solar Energy Conference 2012:1–8.

[38] Cengel YA, Ghajar AJ, Kanoglu M. Heat and mass transfer: fundamentals and applications. (No Title) 2011.

[39] Kanoglu M. Thermodynamics: An Engineering Approach. 8th. Edition in SI Units; 2015.

[40] Sánchez D, Cabello R, Llopis R, Arauzo I, Catalán-Gil J, Torrella E. Energy performance evaluation of R1234yf, R1234ze (E), R600a, R290 and R152a as low-GWP R134a alternatives. Int J Refrig 2017;74:269–82.

[41] Wang F, Gao W, Li G, Tian Z, Wang X. Experimental study on power generation plant of a 1 kW small-scale Organic Rankine Cycle system using R290. Energy Sci Eng 2022;10:740–51.

[42] Cengel YA, Boles MA, Kanoğlu M. Thermodynamics: an engineering approach. McGraw-hill New York; 2011.

[43] Khanmohammadi S, Khanmohammadi S. Energy, exergy and exergo-environment analyses, and tri-objective optimization of a solar still desalination with different insulations. Energy 2019;187:115988.

[44] R. Hogan, R. Diver, W.B. Stine, Comparison of a cavity solar receiver numerical model and experimental data, (1990).